AIAA 2000-2581

Natural Convection from Isothermal Convex Bodies: Simple Models for Bounds on Body-Gravity Function

M.M.Yovanovich
Microelectronics Heat Transfer Laboratory
Department of Mechanical Engineering
University of Waterloo
Waterloo, Ontario, CANADA

34th AIAA Thermophysics Conference
19-22 June 2000 / Denver, CO

NATURAL CONVECTION FROM ISOTHERMAL CONVEX BODIES: SIMPLE MODELS FOR BOUNDS ON BODY-GRAVITY FUNCTION

M.M. Yovanovich†
Microelectronics Heat Transfer Laboratory
Department of Mechanical Engineering
University of Waterloo
Waterloo, Ontario, Canada N2L 3G1
http://www.mhtl.uwaterloo.ca

Abstract

Simple, geometric rules are presented for obtaining bounds for the body-gravity function for laminar boundary layer flow of high Prandtl number fluids over three-dimensional convex isothermal bodies. The upper bound is based on the maximum body perimeter horizontal to the gravity vector. The lower bound for axisymmetric bodies is based on the maximum flow distance, and for nonsymmetric bodies, it is based on the harmonic mean of the maximum flow distances corresponding to the two axes which are perpendicular to the gravity vector. The bounds differ by less than twenty percent for a wide range of body shapes in vertical and horizontal orientations. The lower bound values are close to the theoretical and experimental values with differences of approximately five percent for a wide range of body shapes and orientations.

Nomenclature

A	=	surface area of the body; m^2
$\tilde{A}$	=	area fraction
$\tilde{A}_i$	=	area fraction of the i-th component
$\sqrt{A}$	=	characteristic length of the body; m
$B(x,y)$	=	Beta function
D_{max1}	=	maximum flow distances along axes
D_{max2}		perpendicular to gravity vector; m
D_{max}	=	maximum flow distance; $\left[(D_{max1}^{-1} + D_{max2}^{-1})/2\right]^{-1}$; m
$F(Pr)$	=	Prandtl number function $\left[0.670/[1+(0.50/Pr)^{9/16}]^{4/9}\right]$
g	=	gravitational acceleration; m/s^2
$G_{\sqrt{A}}$	=	laminar boundary layer body-gravity function based on $\sqrt{A}$
$G_{\mathcal{L}}$	=	body-gravity function based on arbitrary body length $\mathcal{L}$
h	=	heat transfer coefficient; $W/m^2{\cdot}K$
k	=	thermal conductivity; $W/m{\cdot}K$
$Nu_{\sqrt{A}}$	=	Nusselt number, $h\sqrt{A}/k$
$P(\theta)$	=	local perimeter; m
P_{max}	=	maximum perimeter perpendicular to gravity vector, m
Pr	=	Prandtl number; ν/α
$Ra_{\sqrt{A}}$	=	Rayleigh number; $\frac{g\beta(T_0-T_\infty)(\sqrt{A})^3}{\alpha\nu}$
$S^*_{\sqrt{A}}$	=	dimensionless shape factor, $S\sqrt{A}/A$
T_∞	=	ambient temperature; K
T_0	=	surface temperature; K
T_f	=	film temperature, $(T_0+T_\infty)/2$; K

Greek Symbols

α	=	thermal diffusivity; $k/\rho c_p$; m^2/s
β	=	volumetric expansion coefficient; K^{-1}
θ	=	angle between gravity vector and outward normal to surface; rad
ν	=	kinematic viscosity, μ/ρ; m^2/s
ρ	=	mass density; kg/m^3
ϕ	=	dimensionless temperature excess, $(T(\mathbf{r})-T_\infty)/(T_0-T_\infty)$

Miscellaneous Symbols

bot	=	bottom surface area of body
rect plate	=	value for rectangular plate
side	=	side surface area of body
top	=	top surface of body
total	=	total surface area of body

Subscripts and Superscripts

$\sqrt{A}$	=	based on $\sqrt{A}$, the characteristic length
D	=	cylinder and sphere diameter
$\tilde{}$	=	dimensionless quantity

† Fellow AIAA, Distinguished Professor Emeritus

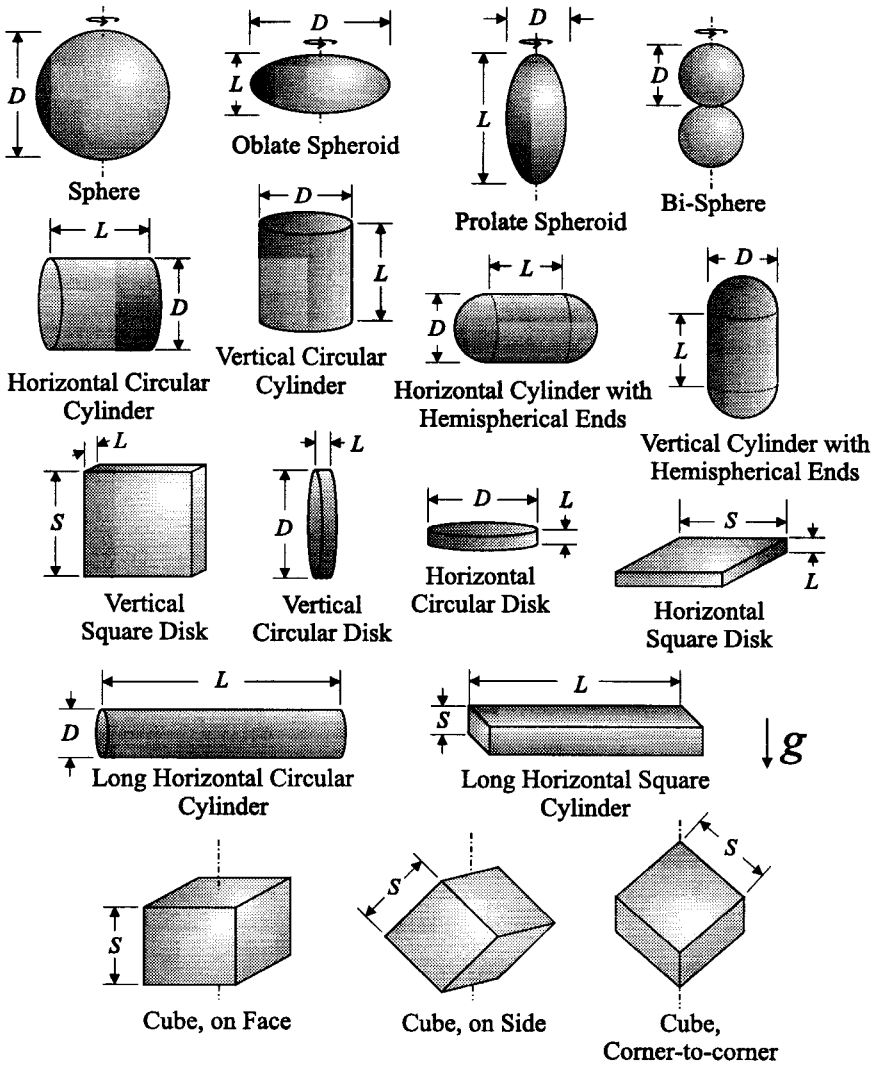

Figure 1: Summary of Body Shapes

Introduction

Steady laminar natural convection from isothermal convex bodies of complex shape, such as those shown in Fig. 1, has been the subject of numerous experimental and theoretical studies. A recent, comprehensive experimental program has reported air data for a wide range of body shapes in different orientations over several decades of the Rayleigh number. Chamberlain[1] and Chamberlain et al.[2] reported air data for spheres, vertical bispheres and cubes in three different orientations. Clemes[3] and Clemes et al.[4] reported air data for horizontal, relatively long cylinders of different cross-sections (circular, square, semi-circular, etc) in different orientations. Hassani[5] and Hassani and Hollands[6] reported air data for a vertical prolate spheroid and horizontal oblate spheroids, finite circular cylinders and disks in vertical and horizontal orientations, circular cylinder with hemispherical ends in vertical and horizontal orientations, and thin square disk in vertical and horizontal orientations. Jafarpur[7] and Yovanovich and Jafarpur[8–10] reported air data for thin horizontal elliptical disks, vertical thin circular disks, thin oblate spheroids and cones facing upward and downward. Several of these body shapes in two orientations are shown in Fig. 1.

Models were proposed by Raithby and Hollands[11,12] for prediction of the Nusselt-Rayleigh relations for different body shapes. The laminar-turbulent model of Raithby and Hollands[11,12] is a multi-step procedure which requires several semi-empirical parameters to be computed. In general they do not provide simple correlation equations.

Jafarpur[10] reviewed the modified Raithby-Hollands model[6] which is also a multi-step proce-

dure requiring several semi-empirical parameters for proper implementation.

Jafarpur[7] also reviewed the simple two term laminar model proposed by Yovanovich[13-15] which is based on the linear superposition of the dimensionless shape factor[16] corresponding to pure conduction from the body and the thin, laminar boundary-layer asymptote which consists of the product of the Prandtl number function, the body-gravity function and the Rayleigh number[13-15].

Lee et al.[17] re-derived the thin, laminar boundary-layer solution and demonstrated that the body length scale which best characterizes the natural convection from isothermal convex bodies is the square root of the active surface area; a length scale first proposed by Yovanovich[13-16].

Jafarpur[7] demonstrated that the Yovanovich model with the appropriate dimensionless shape factor and body-gravity function predicts all air data over the full range of the Rayleigh number with very good to excellent agreement.

Mathematical Problem and Asymptotic Solutions

The mathematical problem statement is based on steady laminar flow of a constant property fluid over an isothermal convex body which is surrounded by a large extent of stationary fluid. The Boussinesq approximation is used for the fluid mass density.

The general natural convection problem is complex because the partial differential equations are nonlinear and coupled (momentum and energy) through the temperature:

Continuity:

$$\nabla \cdot \mathbf{V} = 0 \tag{1}$$

Momentum:

$$(\mathbf{V} \cdot \nabla)\,\mathbf{V} = g\beta\,(T_0 - T_\infty)\,\phi + \nu\,\nabla^2\mathbf{V} \tag{2}$$

Energy:

$$(\mathbf{V} \cdot \nabla)\,\phi = \alpha\nabla^2\phi \tag{3}$$

with dimensionless temperature excess

$$\phi = (T(\mathbf{r}) - T_\infty)\,/\,(T_0 - T_\infty)$$

The thermal-fluid boundary conditions are:

$$\phi = 1, \quad \mathbf{V} = 0$$

at points on the body, and

$$\phi \to 0, \quad \mathbf{V} \to 0,$$

for points remote from the body. The coupled nonlinear equations cannot be solved for a wide range of Prandtl, Grashof and Rayleigh numbers. Approximate analytical methods must be employed to find the dimensionless steady heat transfer rate from the total body surface:

$$\begin{aligned} Q^\star_{\mathcal{L}} &= \frac{Q\mathcal{L}}{k\,(T_0 - T_\infty)\,A} \\ &= \frac{\mathcal{L}}{A}\int\!\!\int_A -\nabla\phi \cdot \mathbf{n}\,dA \\ &= \frac{\mathcal{L}}{A}\int\!\!\int_A -\frac{\partial\phi}{\partial n}\,dA \end{aligned} \tag{4}$$

where $\mathcal{L}$ is some characteristic scale length based on one or more of the body dimensions. In general, the normal gradient $\partial\phi/\partial n$ of the dimensionless temperature at points on the surface of the body varies with position in some complex manner.

If the fluid velocity goes to zero, $\mathbf{V} \to 0$, then $Gr_{\mathcal{L}}$ and $Ra_{\mathcal{L}} \to 0$, and the set of equations reduces to the energy equation only, and it becomes $\nabla^2\phi = 0$ which corresponds to pure conduction from the surface of the isothermal body into the surrounding stationary medium.

The dimensionless heat transfer rate is found from the dimensionless shape factor[16]:

$$Q^\star_{\mathcal{L}} = S^\star_{\mathcal{L}} = \frac{S\mathcal{L}}{A}$$

If the maximum fluid velocity is such that the Grashof number lies in the range $10^4 < Gr_{\mathcal{L}} < 10^{11}$, then the buoyancy-induced flow over the body surface is laminar and it is confined to a very thin hydrodynamic layer attached to the body surface. If the Prandtl number is large, $Pr >> 1$, there is a very thin thermal boundary layer within the hydrodynamic boundary layer. Under these conditions the dimensionless heat transfer rate is called the Nusselt number:

$$Q^\star_{\mathcal{L}} = Nu_{\mathcal{L}} = \frac{h\mathcal{L}}{k}$$

where the area-average heat transfer coefficient is defined as

$$h = \frac{Q}{A\,(T_0 - T_\infty)}$$

Solutions of the governing equations for the full range of Grashof number $0 \le Gr_{\mathcal{L}} < 10^9$ and Prandtl number $0 < Pr < \infty$ are not available for arbitrary three-dimensional convex bodies in arbitrary orientations. The dimensionless heat transfer rate has the following asymptotic relations:

$$Q^\star_{\mathcal{L}} \to S^\star_{\mathcal{L}} \quad \text{as} \quad Gr_{\mathcal{L}} \to 0$$

and

$$Q^*_{\mathcal{L}} \rightarrow Nu_{\mathcal{L}} = C_{\mathcal{L}} Ra^{1/4}_{\mathcal{L}} \quad \text{for} \quad 10^4 < Gr_{\mathcal{L}} < 10^9$$

The coefficient $C_{\mathcal{L}}$ is related to a thermal-fluid boundary layer parameter called the body-gravity function, denoted $G_{\mathcal{L}}$, and a Prandtl number function, $F(Pr)$, that accounts for the interplay between the thermal and hydrodynamic boundary layers. The body-gravity function was developed for $10^4 < Gr_{\mathcal{L}} < 10^9$ and with $Pr \rightarrow \infty$. It depends on the body shape, it's orientation with respect to the gravity vector, and the choice of $\mathcal{L}$. The coefficient was found to have the following asymptotic relations for very small and very large values of the Prandtl number[7,17]:

$$\frac{C_{\mathcal{L}}}{G_{\mathcal{L}}} = \begin{cases} C_0 Pr^{1/4} & \text{for } Pr \rightarrow 0 \\ C_\infty & \text{for } Pr \rightarrow \infty \end{cases}$$

where C_0 and C_∞ are constants.

The Prandtl number function was introduced to *connect* the asymptotic solutions. The *universal* form of the Prandtl number function applicable to a wide range of body shapes was proposed by Churchill and Churchill[18] and recommended by Lee at al.[17]

$$F(Pr) = \frac{0.670}{\left[1 + (0.5/Pr)^{9/16}\right]^{4/9}}, \quad 0 < Pr < \infty \tag{5}$$

This form of the Prandtl number function has the following asymptotic relations[7,17]:

$$F(Pr) = \begin{cases} 0.797 Pr^{1/4} & \text{for } Pr \rightarrow 0 \\ 0.670 & \text{for } Pr \rightarrow \infty \end{cases}$$

To illustrate how the various solutions are *combined* into a comprehensive correlation equation valid for the full range of Prandtl number and the laminar flow range of the Grashof and Rayleigh numbers, the solutions for the isothermal sphere of diameter D will be considered. If the characteristic body length is chosen as $\mathcal{L} = D$, then the asymptotic solutions are:

$$Q^*_D \rightarrow S^*_D = 2, \qquad Gr_D \rightarrow 0 \tag{6}$$

and

$$Q^*_D \rightarrow Nu_D = F(Pr) G_D Ra^{1/4}_D, \quad 10^4 < Gr_D < 10^9 \tag{7}$$

The small and large Prandtl number solutions for thin laminar boundary layers are given as

$$Nu_D = \begin{cases} C_0 G_D Ra^{1/4}_D Pr^{1/4} & \text{for } Pr \rightarrow 0 \\ C_\infty G_D Ra^{1/4}_D & \text{for } Pr \rightarrow \infty \end{cases}$$

where $C_0 = 0.800$ and $C_\infty = 0.670$ are constants.

It was shown that natural convection heat transfer can be predicted accurately by the linear superposition of the solutions for the conduction problem and the laminar thin boundary layer flow. For air ($Pr = 0.71$), $F(Pr) = 0.513$ and with $G_D = 0.878$, the sphere correlation equation becomes:

$$Nu_D = 2 + 0.450\, Ra^{1/4}_D \tag{8}$$

This simple, two-term relation is in excellent agreement with the dry air data of Chamberlain[1,2], for the Rayleigh number range: $10 < Ra_D < 10^8$. The RMS percent difference is about 2.5% and the maximum absolute percent difference is approximately 4%.

Model and General Equation

The general correlation equation for natural convection from isothermal convex bodies into a large stationary medium proposed by Yovanovich[13–15] consists of the linear superposition of the dimensionless shape factor and the thin laminar boundary layer asymptote:

$$Nu_{\mathcal{L}} = S^*_{\mathcal{L}} + F(Pr) G_{\mathcal{L}} Ra^{1/4}_{\mathcal{L}} \tag{9}$$

$$0 \leq Ra_{\mathcal{L}} < 10^{11}, \quad 0 < Pr < \infty$$

The dimensionless shape factor $S^*_{\mathcal{L}}$ is the solution of the three-dimensional Laplace equation $\nabla^2 \phi = 0$ which corresponds to zero values of the Grashof and Rayleigh numbers. Many solutions and methods[16] of finding the dimensionless shape factor are available. The Prandtl number function proposed by Churchill and Churchill[18] and recommended by Lee et al.[17] is used. Methods for finding the body-gravity function for many complex three-dimensional bodies are also available[7–10,13–15,17], and they will be discussed below.

Body-Gravity Function

The body-gravity function developed by Lee, Yovanovich and Jafarpur[17] has the general form:

$$G_{\sqrt{A}} = \left[\frac{1}{A} \int\int_A \left(\frac{P(\theta)}{\sqrt{A}} \sin\theta \right)^{1/3} dA \right]^{3/4} \tag{10}$$

and it is valid for axisymmetric and two-dimensional geometries. The two parameters which make the body-gravity difficult to evaluate symbolically are the local perimeter $P(\theta)$ and $\sin\theta$ which represents the local tangential component of the body force

near the body surface. When the product $P(\theta)\sin\theta$ is discontinuous over portions of the body surface, for example, a horizontal cube or a vertical solid cylinder of finite length, it is necessary to partition the total body surface into component surfaces: the horizontal top and bottom components and the vertical side component. Over the vertical side component $\sin\theta = 1$, and the integration over the side surface can be done with relative ease, while over the horizontal components $\sin\theta$ is zero, and therefore the integrations cannot be accomplished symbolically without introduction of some approximations or empirical information.

Lee, Yovanovich and Jafarpur[17] also presented two rules for application of the theoretical expression, Eq. (10). When N component surfaces of the body are arranged in series flow, then the body-gravity function relation must be employed:

$$G_{\sqrt{A}} = \left[\sum_{i=1}^{N} G_{\sqrt{A}_i}^{4/3}\, \tilde{A}_i^{7/6}\right]^{3/4} \qquad (11)$$

where $G_{\sqrt{A}_i}$ represent the component values of the body-gravity function and $\tilde{A}_i$ represents the area fraction and $\sum_{i=1}^{N} \tilde{A}_i = 1$

For component surfaces arranged in parallel flow, e.g. a horizontal finite circular cylinder with flat ends, the overall body-gravity function is obtained from the relation:

$$G_{\sqrt{A}} = \sum_{i=1}^{N} G_{\sqrt{A}_i}\, \tilde{A}_i^{7/8} \qquad (12)$$

It was demonstrated by Jafarpur[7], Yovanovich and Jafarpur[8-10], and Lee, Yovanovich and Jafarpur[17] that when the relations given above are used to predict natural convection from a wide range of isothermal, convex bodies, the agreement between the theoretical and experimental values is very good to excellent over a wide range of Rayleigh number for $Pr = 0.71$.

Although the relationships given above for the body-gravity function provide accurate predicts, the method is not easy to implement without the aid of Computer Algebra Systems (CAS) such as Maple[19] and Mathematica[20].

The body-gravity function reduces to a simple geometric relation when the body is a vertical, isothermal rectangular plate of height H parallel to the gravity vector, and width W. For this body, $\sin\theta = 1$ over the entire surface, and the body-gravity function, Eq. (10), gives:

$$G_{rect\ plate} = \left[\frac{W}{H}\right]^{1/8} \qquad (13)$$

when heat transfer occurs from one side only. A factor of $2^{1/8}$ appears when both sides of the rectangular plate are active.

Two examples are presented to illustrate the complex analysis required to obtain the body-gravity function. The first example is the isothermal sphere which is representative of axisymmetric bodies such as oblate spheroids and vertical prolate spheroids. The second example is the horizontal, isothermal cube which is representative of bodies which have horizontal surfaces such as vertical finite length circular or elliptical solid cylinders with flat ends. The second example will illustrate the series flow arrangement and the need to partition the total surface area into component parts to calculate the body-gravity function.

Sphere

The determination of the body-gravity function for spheres of diameter D requires the local geometric parameters:

$$P(\theta) = \pi D \sin\theta, \quad dA = \frac{D^2}{4}\sin\theta\, d\theta\, d\psi$$

and the surface area $A = \pi D^2$. The general expression, Eq. (10), becomes

$$G_{\sqrt{A}} = \left[\frac{1}{\pi D^2}\int_0^{2\pi}\int_0^{\pi}\left[\frac{\pi D \sin^2\theta}{\sqrt{\pi}D}\right]^{1/3}\frac{D^2}{4}\sin\theta d\theta d\psi\right]^{3/4}$$

which reduces to

$$G_{\sqrt{A}} = \left[\frac{\pi^{1/6}}{2}\int_0^{\pi}\sin^{5/3}\theta\, d\theta\right]^{3/4}$$

Recognizing that the integral can be represented by the beta function $B(x,y)$[21] allows transformation of the integral and the above expression to the compact form:

$$G_{\sqrt{A}} = \frac{\pi^{1/8}}{2^{3/4}}\left[B(4/3, 1/2)\right]^{3/4}$$

The final result can be evaluated by means of Computer Algebra Systems to find $G_{\sqrt{A}} = 1.014$. This value is within 1.4% of the value for a vertical square plate ($H = W$) having a surface area equal to that of the sphere. It appears that it may be possible to find a close approximate value for the sphere by means of simple geometric rules which map the surface of the sphere on to an equivalent vertical rectangular plate having identical total surface area.

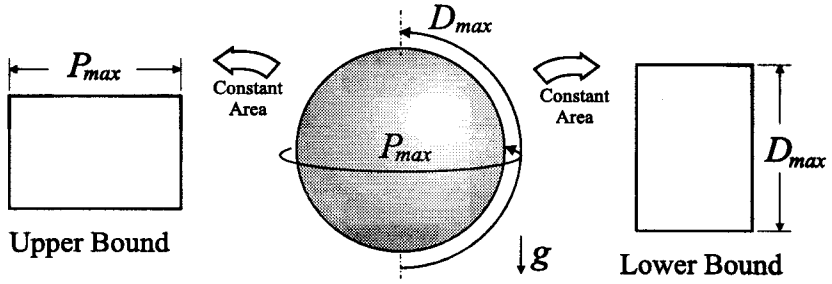

Figure 2: Schematic of Modeling Procedure

Horizontal Cube

A cube of side dimensions s has total surface area $A = 6s^2$, and maximum perimeter perpendicular to the gravity vector $P_{max} = 4s$. The determination of the body-gravity function for the horizontal cube requires the series flow arrangement relation which for the cube is written as:

$$G_{\sqrt{A}} = \left[G_{bot}^{4/3} \tilde{A}_{bot}^{7/6} + G_{side}^{4/3} \tilde{A}_{side}^{7/6} + G_{top}^{4/3} \tilde{A}_{top}^{7/6} \right]^{3/4} \tag{14}$$

The area fraction for the four vertical sides of the cube is $\tilde{A}_{side} = 4/6$, and the area fraction for the horizontal top and bottom surfaces is $\tilde{A}_{top} = \tilde{A}_{bot} = 1/6$. The component body-gravity function for the vertical sides comes directly from Eq. (10). With $\sin\theta = 1$, $G_{sides} = 4^{1/8}$. The body-gravity functions for the horizontal top and bottom surfaces are empirically based[7-10], and they are approximated by the relations: $G_{top} = 2^{1/8}$ and $G_{bot} = G_{top}/2$. Substituting these relations into the series flow arrangement expression gives:

$$\begin{aligned} G_{cube} &= \left[\left(2^{1/8}\right)^{4/3} \left(\frac{1}{6}\right)^{7/6} \right. \\ &\quad + \left(\frac{2^{1/8}}{2}\right)^{4/3} \left(\frac{1}{6}\right)^{7/6} \\ &\quad \left. + \left(4^{1/8}\right)^{4/3} \left(\frac{4}{6}\right)^{7/6} \right]^{3/4} \\ &= 0.984 \end{aligned} \tag{15}$$

This numerical value has been confirmed by means of the air data of Chamberlain[1,2] and the comparison is reported in Lee et al.[17] The computed value of the body-gravity function for the cube is approximately 3% smaller than the value for a sphere having identical total surface area, and it is approximately 1.6% smaller than the value for the vertical square plate having identical total surface area. The close relationships between the vertical square plate, sphere and horizontal cube suggests that it may be possible to develop methods for obtaining approximate values for the body-gravity functions of other convex bodies.

To obtain numerical values of the body-gravity function for other body shapes such as oblate and prolate spheroids, and horizontal thin elliptical disks requires evaluations of complex integrals which often lead to special functions such as incomplete elliptic integrals[21] which frequently require numerical computations.

There is clearly a requirement to find a simpler method of estimating the body-gravity function for all isothermal convex bodies. In the subsequent section, simple rules will be established for obtaining upper and lower bounds for the body-gravity function by means of certain geometric characteristics of the body such as the maximum perimeter perpendicular to the gravity vector, and the maximum fluid flow distance over the body.

Bounds for the Body-Gravity Function

The schematic in Fig. 2 illustrates how bounds can be established with the sphere as the example of a three-dimensional convex body. The simple relation for the body-gravity function for the vertical rectangular plate will be used to establish bounds for the body-gravity function, Eq. (10), for a range of body shapes and orientations. The surface area of the equivalent rectangular plate HW will be set equal to the total surface area of the body A such that $HW = A$.

An Upper Bound

An upper bound on the body-gravity function is found by setting the width of the equivalent vertical rectangular plate equal to the maximum perimeter of the body:

$$W_{max} = P_{max} \tag{16}$$

The corresponding minimum height of the equiva-

lent rectangle is found from the area equality:

$$H_{min} = \frac{A}{W_{max}} \tag{17}$$

This simple procedure maps the surface of a given convex body on to a vertical rectangular plate with the largest width and the smallest height. The body-gravity function for this rectangular plate should have body-gravity function values which are greater than the true value for the body of interest.

Substituting the relations into the body-gravity function for the rectangular plate gives a simple upper bound relation for all three-dimensional convex bodies:

$$G_{upper\ bound} = \left[\frac{P_{max}^2}{A}\right]^{1/8} = \left[\frac{P_{max}}{\sqrt{A}}\right]^{1/4} \tag{18}$$

A very simple relation has been found for an upper bound on the body-gravity function. It is based on two body geometric parameters which are easily found for all three-dimensional bodies.

A Lower Bound

A lower bound on the body-gravity function is obtained by setting the height of the equivalent rectangular plate equal to the maximum flow distance from the lowest stagnation point to the highest point on the surface of the body as shown in Fig. 2. For axisymmetric bodies shown in Fig. 1, such as vertical prolate spheroids, oblate spheroids and vertical cylinders of constant cross-section, the maximum flow distance is relatively simple to find. For non-symmetric horizontal bodies shown in Fig. 1, such as cuboids (e.g. cube), circular cylinders with flat ends or hemispherical ends, and vertical circular and square disks, there are two possible maximum flow distances corresponding to the two axes. Let the two possible maximum flow distances be denoted as D_{max1} and D_{max2}. These two relations can be combined in the following manner to get the effective maximum flow distance:

$$D_{max} = \left[\frac{1}{2}\left(\frac{1}{D_{max1}} + \frac{1}{D_{max2}}\right)\right]^{-1} \tag{19}$$

This definition of the effective maximum flow distance will ensure that D_{max} will approach the value of the smaller value of D_{max1} and D_{max2} for long horizontal circular and square cylinders. The maximum height of the equivalent vertical rectangular plate is found from the relation:

$$H_{max} = D_{max} \tag{20}$$

The corresponding minimum width of the equivalent rectangular plate is found from the area equality:

$$W_{min} = \frac{A}{H_{max}} \tag{21}$$

This simple procedure produces a vertical rectangular plate which has the greatest height and the smallest width. The body-gravity function value for this rectangular plate is expected to be comparable or smaller than the true value of the body-gravity function for the given body. When the body has horizontal surfaces and they represent a significant fraction of the total surface, this procedure may not give acceptable values.

Substituting the relations into the body-gravity function for the rectangular plate gives a lower bound relation:

$$G_{lower\ bound} = \left[\frac{A}{D_{max}^2}\right]^{1/8} = \left[\frac{\sqrt{A}}{D_{max}}\right]^{1/4} \tag{22}$$

A simple relation has been found for a lower bound on the body-gravity function which is also based on two geometric parameters of the body which can be found easily for all three-dimensional convex bodies.

Bounds for Vertical and Horizontal Bodies

The body-gravity function for any convex body is expected to be related in some manner to the established bounds which are obtained through simple rules from the geometric characteristics of the body. The upper and lower bound relations given above will be used to find bounds for several finite length bodies in vertical and horizontal orientations with respect to the gravity vector. The study begins with the sphere.

Sphere

The total surface area is $A = \pi D^2$, the maximum perimeter perpendicular to the gravity vector is $P_{max} = \pi D$ and the maximum particle flow distance from pole to pole is $D_{max} = \pi D/2$. The upper and lower bounds values are found to be $G_{UB} = 1.1538$ and $G_{LB} = 1.0307$ which differ by approximately 12%. The theoretical and experimental values[7,14,15,17] are $G_{theo} = 1.014$ and $G_{expt} = 1.023$ respectively. The theoretical value is approximately 1.6% smaller than the lower bound value.

Vertical Prolate Spheroid

The vertical prolate spheroid has semi-axes: a, b with $a \geq b$. The major axis is parallel to the gravity vector as shown in Fig. 1. The maximum perimeter

is $P_{max} = 2\pi b$ and the maximum flow distance is given by

$$D_{max} = 2aE\left(\sqrt{1-\frac{b^2}{a^2}}\right) \qquad (23)$$

where $E(\kappa)$[21] is the complete elliptic integral of the second kind of modulus κ. The surface area is obtained from

$$A = 2\pi b^2\left[1+\frac{a/b}{\sqrt{1-b^2/a^2}}\sin^{-1}\sqrt{1-b^2/a^2}\right],$$

$$0 < \frac{b}{a} \leq 1$$

For a prolate spheroid with $a/b = 1.93$, the upper and lower bound values are found to be $G_{UB} = 1.083$ and $G_{LB} = 0.992$. The upper and lower bound values differ by approximately 9%. The theoretical and experimental values[7,15,17] are $G_{theo} = 1.003$ and $G_{expt} = 1.012$. The agreement between the lower bound value and the theoretical and experimental values are within 2%.

Vertical Oblate Spheroid

The vertical oblate spheroid has semi-axes: a, c with $c \leq a$. The minor axis is parallel to the gravity vector as shown in Fig. 1. The maximum perimeter is $P_{max} = 2\pi a$ and the maximum flow distance is

$$D_{max} = 2aE\left(\sqrt{1-\frac{c^2}{a^2}}\right)$$

The surface area is obtained from

$$A = 2\pi a^2\left[1+\frac{(c/a)^2}{\sqrt{1-c^2/a^2}}\cosh^{-1}\frac{a}{c}\right]$$

For the oblate spheroid with $c/a = 0.5$, the upper and lower bound values are found to be $G_{UB} = 1.209$ and $G_{LB} = 1.050$. The theoretical and experimental values[7,15,17] are $G_{theo} = 0.954$ and $G_{expt} = 0.973$. The upper and lower bound values differ by approximately 15%. The theoretical and experimental values differ by approximately 2%. The lower bound value and the theoretical and experimental values differ by approximately 10% and 7.9% respectively.

Horizontal Cube

The horizontal cube of side dimension s shown in Fig. 1 has total surface area $A = 6s^2$ and maximum perimeter $P_{max} = 4s$. There are two maximum particle flow distances. The shorter maximum particle flow distance is the distance from the midpoint of the lower face to the midpoint of one edge plus the distance up one side plus the distance from the midpoint of the corresponding edge to the midpoint of the top face. This maximum flow distance is $D_{max1} = 2s$. The longer maximum particle flow distance is the distance from the midpoint of the lower face to a corner plus the distance along an edge connecting the lower and upper surfaces plus the distance from the corner to the midpoint of the upper surface. This maximum flow distance is $D_{max2} = (\sqrt{2}+1)\,s$. The upper bound value is $G_{UB} = 1.131$. There are three possible values of the lower bound corresponding to the two maximum flow distances given above, and maximum distance which is based on the harmonic mean of these two maximum flow distances. The three values of the lower bound are $G_{LB} = 1.004, G_{LB} = 1.052$ and $G_{LB} = 1.029$. The third value is recommended. It lies approximately 9.9% below the upper bound value.

The upper and lower bound values are compared against the theoretical and experimental values[7,15,17], $G_{theo} = 0.984$ and $G_{expt} = 0.951$, respectively in Table 1. The theoretical value lies below the lower bound value and it is approximately 4.6% smaller. The calculated lower bound value is not a true lower bound for the horizontal cube.

Cube On Side

The cube on its side (see Fig. 1) has four faces which are inclined to the gravity vector and two faces which are parallel to the gravity vector. The cube in this orientation is representative of a complex convex body. For this orientation where the diagonal connecting two edges is parallel to the gravity vector, $P_{max} = 2(1+\sqrt{2})s$, and $D_{max1} = 2s$ and $D_{max2} = (1+2\sqrt{2})s$. According to the proposed transformation rules the upper and lower bound values are $G_{UB} = 1.185$ and $G_{LB} = 0.983$ which differ by approximately 20%. These values are compared with the theoretical value[7,15,17], $G_{theo} = 1.080$ and the experimental value[7,15,17], $G_{expt} = 0.990$ in Table 1. The reported theoretical value appears to be too large, however the experimental value is within 1% of the calculated lower bound value.

Cube On Corner

The cube oriented such that the gravity vector is parallel to one of its corner-to-corner diagonals as shown in Fig. 1 has all six faces inclined to the gravity vector. This orientation is also representative of a complex convex body with complex fluid flow over its six faces. For this orientation where the diagonal connecting two opposite corners

is parallel to the gravity vector, $P_{max} = 4s$, and $D_{max1} = D_{max2} = (1+\sqrt{2})s$. According to the established rules the upper and lower bound values are $G_{UB} = 1.130$ and $G_{LB} = 1.004$ which differ by approximately 13%. These values compare with the theoretical value[7,15,17], $G_{theo} = 1.091$ and the experimental value[7,15,17], $G_{expt} = 1.014$. The theoretical value appears to be too large; however, the experimental value is within 1.5% of the calculated lower bound value.

Vertical Finite Length Circular Cylinder

The vertical finite length circular cylinder with flat ends has length L equal to the diameter D. The maximum perimeter is $P_{max} = \pi D$ and the maximum particle flow distance is $D_{max} = D + L$. The upper bound value, $G_{UB} = 1.097$, and the lower bound value, $G_{LB} = 1.021$, differ by approximately 7.5%. The theoretical value of the body-gravity function which is based on the series flow arrangement and the following relations for the component values of the body-gravity function:

$$G_{top} = 2^{1/8},\ G_{top} = \frac{1}{2}G_{top},\ G_{side} = \pi^{1/8}\left(\frac{D}{L}\right)^{1/8}$$

is given by the relation:

$$G_{\sqrt{A}} = \pi^{1/8}\frac{(0.2571 + L/D)^{3/4}}{(0.500 + L/D)^{7/8}}, \qquad L/D \geq 0 \tag{24}$$

For $L = D$ the theoretical value is $G_{theo} = 0.961$ which is approximately 5.9% smaller than the lower bound value. The agreement between the theoretical and experimental values is excellent.

Horizontal Finite Length Circular Cylinder

The horizontal circular cylinder has the maximum perimeter $P_{max} = 2(D + L)$ which lies in the plane perpendicular to the gravity vector. The maximum flow distance is based on the two relations: $D_{max1} = \pi D/2$ and $D_{max2} = D + L$. Substitution of the relation $L = D$ into the upper and lower bound relations gives the upper bound value, $G_{UB} = 1.165$, and the lower bound value, $G_{LB} = 1.054$, which differ by approximately 11%. The two circular end surfaces and the circular side surface are in the parallel flow arrangement. The following component body-gravity functions are recommended:

$$G_{end} = 1.021 \quad \text{for each end}$$

and

$$G_{side} = 0.900\left(\frac{L}{D}\right)^{1/8}$$

Using the parallel flow arrangement relation leads to the following expression for the theoretical value:

$$G_{\sqrt{A}} = 0.900\frac{(2/3 + L/D)}{(0.5 + L/D)^{7/8}}, \qquad L/D \geq 0 \tag{25}$$

The theoretical value for the body-gravity function is $G_{theo} = 1.052$ which is approximately 2.9% greater than the lower bound value.

Circular Disk: Axis Horizontal

The circular disk of length $L = 0.1D$ with axis horizontal is shown in Fig. 1. The relations given above for the horizontal finite circular cylinder are used to find the upper and lower bound values of the body-gravity function: $G_{UB} = 1.125$ and $G_{LB} = 1.015$ which differ by approximately 11%. The theoretical value $G_{theo} = 1.079$ is approximately 6.3% greater than the lower bound value. The experimental value $G_{expt} = 1.016$[7,15,17] is in very close agreement with the lower bound value.

Vertical Bispheres

The vertical bispheres consist of two tangent spheres of diameter D, one above the other as shown in Fig. 1. The maximum perimeter is $P_{max} = \pi D$ and the maximum flow distance from the south pole of the lower sphere to the north pole of the upper sphere is $D_{max} = \pi D$. The upper bound, $G_{UB} = 1.058$, and the lower bound, $G_{LB} = 0.945$ differ by approximately 12%. The theoretical value $G_{theo} = 0.930$ lies approximately 1.6% below the lower bound value. The experimental value, $G_{expt} = 0.928$, is in very good agreement also.

Horizontal Bisphere

The horizontal bisphere consists of two tangent spheres of diameter D which lie in a plane which is perpendicular to the gravity vector. The maximum perimeter is $P_{max} = 2\pi D$ and the maximum flow distance is based on the two particle flow distances: $D_{max1} = \pi D/2$ and $D_{max2} = \pi D$. The upper bound, $G_{UB} = 1.258$, and the lower bound, $G_{LB} = 1.046$, differ by approximately 20%. The theoretical value $G_{theo} = 1.106$ lies approximately 5.7% above the lower bound value. The experimental value is not available.

Vertical Circular Cylinder with Hemispherical Ends

The vertical circular cylinder of length L has hemispherical ends of diameter D as shown in Fig. 1. The total surface area is

$$A = \pi DL + \pi D^2$$

Table 1: Summary of Values of Body-Gravity Function

Body, Orientation	G_{UB}	G_{LB}	G_{theo}	G_{expt}
Sphere	1.154	1.031	1.014	1.023
Prolate Spheroid, 1.93:1, major axis vertical	1.083	0.992	1.003	1.012
Oblate Spheroid, 1:2, minor axis vertical	1.209	1.050	0.954	0.973
Bisphere, 2:1, axis vertical	1.058	0.945	0.930	0.928
Bisphere, axis horizontal	1.258	1.046	1.106	n.a.
Cylinder-Flat, 1:1, axis vertical	1.097	1.021	0.961	0.967
Cylinder-Flat, axis horizontal	1.165	1.054	1.052	1.019
Cylinder-Hem., 2:1, axis vertical	1.058	0.994	0.995	1.012
Cylinder-Hem., axis horizontal	1.197	1.065	1.039	1.049
Cube, face horizontal	1.131	1.029	0.984	0.951
Cube, edge horizontal	1.185	0.983	1.080	0.990
Cube, corner-corner vertical	1.130	1.004	1.091	1.014
Cir. Disk, $L = 0.1D$, axis horizontal	1.125	1.015	1.079	1.016
Sq. Disk, $L = 0.1S$, side horizontal	1.092	1.022	1.088	1.039
Sq. Disk, $L = 0.1S$, corner-corner vertical	1.183	0.974	1.048	1.058
Long Sq. Cyl., $L = 10.13S$, horizontal	1.359	1.178	1.163	n.a.
Long Cir. Cyl., $L = 10.23D$, horizontal	1.402	1.204	1.230	n.a.

The maximum perimeter is $P_{max} = \pi D$ and the maximum flow distance is $D_{max} = \pi D/2 + L$. The upper bound $G_{UB} = 1.058$ and the lower bound $G_{LB} = 0.994$ differ by approximately 6.4%. The following theoretical body-gravity function relation is based on the series flow arrangement:

$$G_{\text{vert cyl}} = 1.014 \frac{(1 + 1.188L/D)^{3/4}}{(1 + L/D)^{7/8}}, \qquad (26)$$

$$0 \leq \frac{L}{D} < \infty$$

The theoretical value $G_{theo} = 0.995$ and the lower bound value are in excellent agreement. The experimental value $G_{expt} = 1.012$ is also close to the lower bound value.

Horizontal Circular Cylinder with Hemispherical Ends

The horizontal circular cylinder of length L has hemispherical ends of diameter D as shown in Fig. 1. The maximum perimeter in the plane perpendicular to the gravity vector is $P_{max} = 2L + \pi D$ and the maximum flow distance is based on the two maximum flow distances: $D_{max1} = \pi D/2$ and $D_{max2} = L + \pi D/2$. The upper bound $G_{UB} = 1.197$ and the lower bound $G_{LB} = 1.065$ differ by approximately 12.4%.

The theoretical body-gravity function is based the parallel flow arrangement; it is given by the relation:

$$G_{\text{hor cyl}} = \frac{(1.014 + 0.891L/D)}{(1 + L/D)^{7/8}}, \qquad 0 \leq \frac{L}{D} < \infty \qquad (27)$$

The theoretical value $G_{theo} = 1.039$ is approximately 2.5% smaller than the lower bound value. The experimental value $G_{expt} = 1.049$ is also close to the lower bound value.

Horizontal Long Circular Cylinder

The horizontal long circular cylinder with $L/D = 10.23$ shown in Fig. 1 will be used to verify the proposed method of finding bounds. In this case the relations given above for the finite horizontal cylinder can be used. The upper bound value $G_{UB} = 1.402$, and the lower bound value $G_{UB} = 1.205$ differ by approximately 15%. The corresponding theoretical value $G_{theo} = 1.230$ is within 2.1% of the lower bound value. The experimental value is not available.

Horizontal Long Square Cylinder

The horizontal long square cylinder of length-to-side ratio $L/S = 10.13$ shown in Fig. 1 will also be used to verify the proposed method of finding bounds. In this case the relations given above for the finite horizontal square cylinder can be used. The maximum perimeter is $P_{max} = 2(L+S)$, and the two maximum flow distances are $D_{max1} = 2S$ and $D_{max2} = L + S$. The upper bound value $G_{UB} = 1.359$, and the lower bound value $G_{LB} = 1.178$ differ by approximately 15%.

The theoretical value for the long square cylinder with two sides horizontal is given by the relation:

$$G_{\text{sq. cyl.}} = 2^{1/8} \left\{ \frac{\left[0.625 \left(\frac{L}{S}\right)^{4/3} + \left(1 + \frac{L}{S}\right)^{4/3} \right]^{3/4}}{\left(1 + 2\frac{L}{S}\right)^{7/8}} \right\} \tag{28}$$

The corresponding theoretical value $G_{theo} = 1.163$ is approximately 1.3% smaller than the lower bound value. The experimental value is not available. All calculated values for the two bounds, the theoretical and experimental values are given in Table 1. In Table 1, for cubes: C denotes corner-to-corner orientation, H denotes horizontal orientation, and S denotes from side-to-side orientation. The symbols H and V denote horizontal and vertical orientations respectively. Also n.a. denotes not available.

Summary and Discussion

Two simple rules are presented for finding approximations for the body-gravity function based on the vertical rectangular plate result for three-dimensional convex bodies in vertical and horizontal orientations.

The first rule sets the width of the equivalent rectangle equal to the maximum perimeter of the body perpendicular to the gravity vector, and the height is found from the area equivalence. The first rule provides a true upper bound for the body-gravity function because all values are greater than the theoretical and experimental values. The upper bound values are approximately 6% to 20% greater than the lower bound values.

The second rule sets the height of the equivalent rectangular plate equal to the maximum flow distance from the lowest point to the highest point on the body when the body is axisymmetric such as vertical spheroids and cylinders. For non-axisymmetric bodies such as horizontal cylinders, the maximum flow distance is based on the harmonic mean of the two maximum flow distances corresponding to the two axes of the horizontal body which are perpendicular to the gravity vector. The second rule is not a true lower bound; it, however, provides lower estimates of the body-gravity function, and the values are found to be close to the theoretical and experimental values for a range of body shapes and orientations. The lower bound values are found to be within ±5% of the theoretical and experimental values.

The body-gravity functions of all three-dimensional convex bodies shown in Fig. 1 can be estimated with acceptable accuracy by means of the lower bound rule. The theoretical and available experimental values fall above and below the lower bound values. The largest difference is less than 8%, and the average percent difference is less than 3%. From Table 1 we observe that the lower bound values for all bodies (except the horizontal long circular and square cylinders) lie in the relatively narrow range: $0.945 \leq G_{LB} \leq 1.065$. The difference between the largest and smallest values is approximately 12.7%.

Since the lower bound rule provides acceptable engineering approximations of the body-gravity function for a wide range of convex bodies in the vertical and horizontal orientations, it is recommended for all three-dimensional bodies except those which are horizontal and thin. The following general correlation equation for natural convection from isothermal convex bodies is proposed:

$$Nu_{\sqrt{A}} = S^*_{\sqrt{A}} + F(Pr) \left(\frac{\sqrt{A}}{D_{max}}\right)^{1/4} Ra^{1/4}_{\sqrt{A}} \tag{29}$$

for the ranges:

$$0 \leq Ra_{\sqrt{A}} < 10^{11} \quad \text{and} \quad 0 < Pr < \infty$$

The effective maximum particle flow distance is obtained from the relation:

$$\frac{1}{D_{max}} = \frac{1}{2}\left[\frac{1}{D_{max1}} + \frac{1}{D_{max2}}\right]$$

where D_{max1}, D_{max2} represent two estimates of the maximum particle flow distance corresponding to the two axes of the body. If one of the two values is much larger than the other, say $D_{max2} >> D_{max1}$, then $D_{max} \rightarrow D_{max1}$ which is the smaller maximum flow distance.

If the body is axisymmetric (e.g., oblate and prolate spheroids, sphere and vertical circular cylinders), then $D_{max1} = D_{max2}$. This correlation equation is expected to give values of the Nusselt number

which are accurate to within ±5% of the experimental values based on the results reported in Table 1.

If we consider air with $Pr = 0.71$ and $F(Pr) = 0.513$, and if we take the average value of all values of the body-gravity functions (except the values for the long circular and square cylinders) reported in Table 1, then the Nusselt-Rayleigh number relation can be approximated by

$$Nu_{\sqrt{A}} = S^*_{\sqrt{A}} + 0.52Ra^{1/4}_{\sqrt{A}} \qquad (30)$$

which is consistent with the observations made by Lienhard[22] and Yovanovich[15]. The theoretical relations for the body-gravity function are also presented for several convex bodies.

The proposed rules should not be applied to horizontal thin bodies such as the circular and square disks shown in Fig. 1. Further work is required to establish a simple procedure for estimating body gravity functions for thin horizontal convex bodies.

Acknowledgments

The author acknowledges the continued financial support of the Natural Sciences and Engineering Research Council of Canada. The assistance of P. Teertstra for the preparation of the figures and the formatting of the paper is greatly appreciated.

References

[1]Chamberlain, M.J., " Free Convection Heat Transfer from a Sphere, Cube, and Vertically Aligned Bi-Sphere," M.A.Sc. Thesis, Department of Mechanical Engineering, University of Waterloo, Waterloo, Ontario, 1983.

[2]Chamberlain, M.J., Hollands, K.G.T., and Raithby, G.D.,"Experiments and Theory on Natural Convection Heat Transfer from Bodies of Complex Shape," *J. Heat Transfer*, Vol. 107, 1985, pp. 624-629.

[3]Clemes, S.B., "Free Convection Heat Transfer From Two-Dimensional Bodies," M.A.Sc. Thesis, Department of Mechanical Engineering, University of Waterloo, Waterloo, Ontario, 1990.

[4]Clemes, S.B., Hollands, K.G.T., and Brunger, A.P., "Natural Convection Heat Transfer from Long Horizontal Isothermal Cylinders", *J. of Heat Transfer*, Vol. 116, February, 1994, pp. 97-104.

[5]Hassani, A.V., "An Investigation of Free Convection Heat Transfer from Bodies of Arbitrary Shape," Ph.D. Thesis, Department of Mechanical Engineering, University of Waterloo, Waterloo, Ontario, 1987.

[6]Hassani, A.V. and Hollands, K.G.T., "On Natural Convection Heat Transfer From Three-Dimensional Bodies of Arbitrary Shape," *J. of Heat Transfer*, Vol. 111, 1989, pp. 365-371.

[7]Jafarpur, K., "Analytical and Experimental Study of Laminar Free Convection Heat Transfer From Isothermal Convex Bodies of Arbitrary Shape," Ph.D. Thesis, Department of Mechanical Engineering, University of Waterloo, Waterloo, Ontario, 1992.

[8]Yovanovich, M.M. and Jafarpur, K., "Bounds on Laminar Natural Convection From Isothermal Disks and Finite Plates of Arbitrary Shape For All Orientations and Prandtl Numbers," ASME HTD-Vol. 264, *Fundamentals of Natural Convection*, 1993, pp. 93–110.

[9]Yovanovich, M.M. and Jafarpur, K., "Models of Laminar Natural Convection From Vertical and Horizontal Isothermal Cuboids For All Prandtl Numbers and All Rayleigh Numbers Below 10^{11}," ASME HTD-Vol. 264, *Fundamentals of Natural Convection*, 1993, pp. 111–126.

[10]Yovanovich, M.M. and Jafarpur, K., "Natural Convection from Horizontal Isothermal Elliptical Disks: Models and Experiments," AIAA-97-0593, 35th Aerospace Sciences Meeting & Exhibit, January 6-10, 1997, Reno, NV.

[11]Raithby, G.D. and Hollands, K.G.T., "A General Method of Obtaining Approximate Solutions to Laminar and Turbulent Free Convection Problems," *Advances in Heat Transfer*, Vol. 11, Academic, New York, 1975.

[12]Raithby, G.D. and Hollands, K.G.T, "*Handbook of Heat Transfer*, edited by W.M. Rohsenow, J.P. Hartnett, and Young Cho, McGraw-Hill, New York, 1998, Chap. 4.

[13]Yovanovich, M.M., "New Nusselt and Sherwood Numbers for Arbitrary Isopotential Bodies at Near Zero Peclet and Rayleigh Numbers," AIAA-87-1643, 1987, *AIAA 22nd Thermophysics Conference*, Honolulu, Hawaii.

[14]Yovanovich, M.M., "Natural Convection From Isothermal Spheroids in the Conductive to Laminar Flow Regimes," AIAA-87-1587, 1987, *AIAA 22nd Thermophysics Conference*, Honolulu, Hawaii.

[15]Yovanovich, M.M., "On the Effect of Shape, Aspect Ratio and Orientation Upon Natural Convection From Isothermal Bodies of Complex Shapes," 1987, *ASME National Heat Transfer Conference*, Pittsburg, PA.

[16]Yovanovich, M.M., " A General Expression for Predicting Conduction Shape Factors," *AIAA Prog. in Astro. and Aeronautics: Thermophysics and Spacecraft Control*, Vol. 35, ed. R.G. Hering, MIT Press, Cambridge, MA., 1974, pp. 265-291.

[17]Lee, S., Yovanovich, M.M. and Jafarpur, K., "Effects of Geometry and Orientation on Laminar Natural Convection From Isothermal Bodies," *J. Thermophysics and Heat Transfer*, Vol. 5, 1991, pp. 208-216.
[18]Churchill, S.W. and Churchill, R.U., "A Comprehensive Correlating Equation for Heat and Component Transfer by Free Convection," *AIChE J.*, Vol. 21, 1975, 604-606.
[19]*Maple* Release 5, 1984-1998, Waterloo Maple Software.
[20]*Mathematica*, Version 3.0, 1987-1998, Wolfram Research.
[21]Abramowitz, M. and Stegun, A., *Handbook of Mathematical Functions*, Dover Publications, Inc., 1970, New York, NY.
[22] Lienhard, J.H., "On the Commonality of Equations for Natural Convection From Immersed Bodies," *Int. J. Heat Mass Transfer*, Vol. 16, 1973, pp. 2121-2123.